[10] Luo Y, Chu QX, Zhu L. A miniaturized wide-beanwidth circularly-polarized planar antenna via two pairs of parallel dipoles in a square contour. *IEEE Trans Antennas Propagat.* 2015;63:3753–3759.

[11] Liu N-W, Zhu L, Choi W-W. A low-profile wide-beamwidth circularly-polarized patch antenna on a suspended substrate. *IET Microw Antennas Propagat.* 2016;10:885–890.

[12] Baik J-W, Lee K-J, Yoon W-S, Lee T-H, Kim Y-S. Circularly polarized printed crossed dipole antennas with broadband axial ratio. *Electron Lett.* 2008;44:785–786.

How to cite this article: Zheng D-Z, Luo Y, Chu Q-X. Axial-ratio beamwidth and gain enhanced circularly polarized antenna using parasitic elements. *Microw Opt Technol Lett*. 2017;59:2922–2929. https://doi.org/10.1002/mop.30851

Received: 15 April 2017

DOI: 10.1002/mop.30848

Dual-wideband band pass filter using folded cross-stub stepped impedance resonator

Teguh Firmansyah[1] | **Supriyanto Praptodinoyo**[1] | **Romi Wiryadinata**[1] | **Suhendar Suhendar**[1] | **Siswo Wardoyo**[1] | **Alimuddin Alimuddin**[1] | **Cindy Chairunissa**[2] | **Mudrik Alaydrus**[3] | **Gunawan Wibisono**[4]

[1] Department of Electrical Engineering, University of Sultan Ageng Tirtayasa, Cilegon, Banten 42435, Indonesia

[2] School of Engineering, Electronics, University of Edinburgh, Edinburgh EH9 3JN, United Kingdom

[3] Department of Electrical Engineering, Universitas Mercu Buana, Meruya, Jakarta 11650, Indonesia

[4] Department of Electrical Engineering, Universitas Indonesia, Kampus Baru UI, Depok 16424, Indonesia

Correspondence
Teguh Firmansyah, Department of Electrical Engineering, University of Sultan Ageng Tirtayasa, Cilegon, Banten 42435, Indonesia.
Email: teguhfirmansyah@untirta.ac.id

Abstract

In this letter, a dual-wideband band pass filter (DW-BPF) using cross-stub stepped impedance resonator (CS-SIR) was simulated, fabricated, and measured accordingly. The CS-SIR was used to replace the conventional half-wavelength open stub resonators. Compare to the conventional resonator, the CS-SIR resonator has a wider fractional bandwidth and ease of fabrication. Furthermore, the DB-BPF was fabricated on microstrip with $\varepsilon_r = 4.4$, $h = 0.8$ mm, and tan $\delta = 0.0265$. The DW-BPF with CS-SIR achieves transmission-coefficients/fractional-bandwidth of 0.22 dB/94.19% and 1.87 dB/33.52% at 1.14 GHz and 2.31 GHz, respectively. In order to reduce the filter size, a folded CS-SIR (FCS-SIR) was also proposed. As a result, this BPF size was reduced to 53%, with the BPF size of 0.30 λ_G^2 and 0.14 λ_G^2 for DW-BPF with CS-SIR and DW-BPF with folded CS-SIR, respectively. The λ_G is the wavelength at the first frequency. Further, the DW-BPF with FCS-SIR achieves transmission coefficients/fractional bandwidth of 0.19 dB/89.08% and 1.29 dB/31.90% at 1.21 GHz and 2.41 GHz, respectively. Measured results are in a very good agreement with the simulated results.

KEYWORDS

dual-wideband band pass filter, stepped impedance resonator, transmission zero

1 | INTRODUCTION

A dual-band band pass filter (DB-BPF) is an important component of a radio transceiver for reducing interference and noise at two frequency bands simultaneously.[1] Therefore, the pursuit of a DB-BPF with good-performances has become a key trend in the field of research. A variety of design

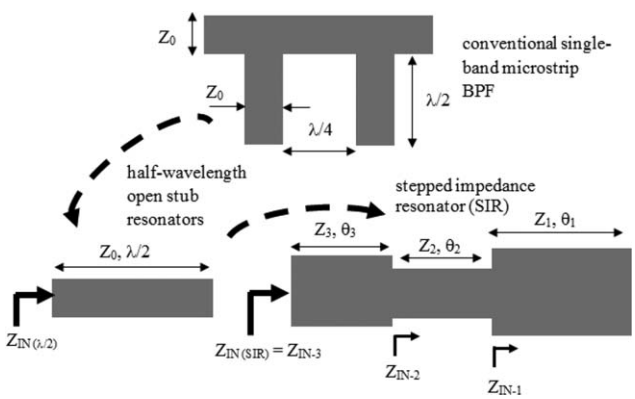

FIGURE 1 The conventional half-wavelength open stub resonator replaced by stub-stepped impedance resonator

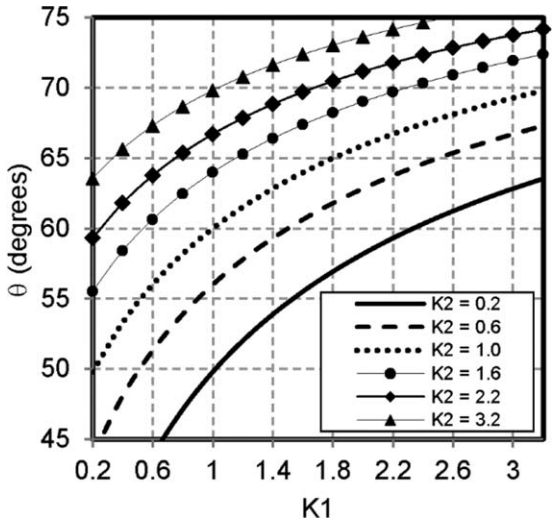

FIGURE 2 The relationship between impedance ratio (K_1, K_2) and electrical length (θ)

techniques is frequently used for DB-BPF design such as square loop dual mode resonator,[2] defected ground structure (DGS),[3,4] spiral resonators,[5] defected stepped impedance resonator (Defected-SIR),[6,7] slotted stepped impedance resonator (Slotted-SIR),[8] multilayer stepped impedance resonator (Multilayer-SIR),[9,10] meandering stepped impedance resonators (Meandering-SIR),[11] stub-loaded stepped impedance resonator (Stub-loaded SIR),[12] and coupled stepped impedance resonator (Coupled-SIR).[13] However, the DB-BPFs proposed by[1–13] still possess a complex geometry and achieve a narrow bandwidth.

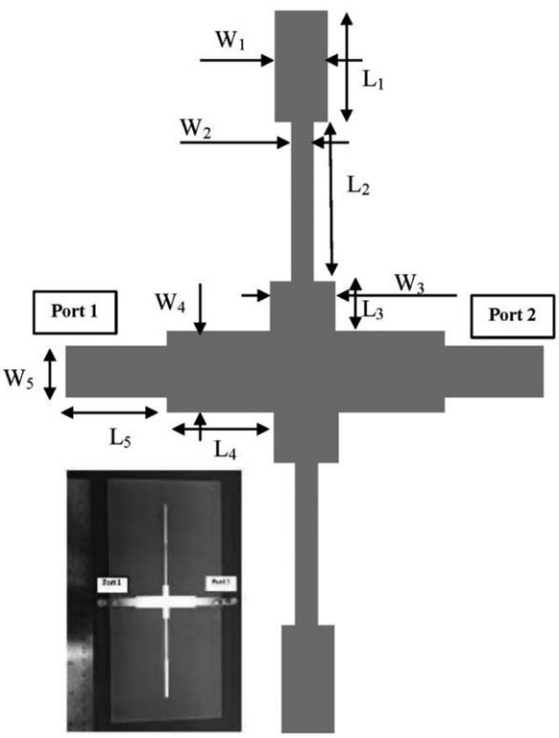

FIGURE 3 The layout and photograph of the design DW-BPF using CS-SIR

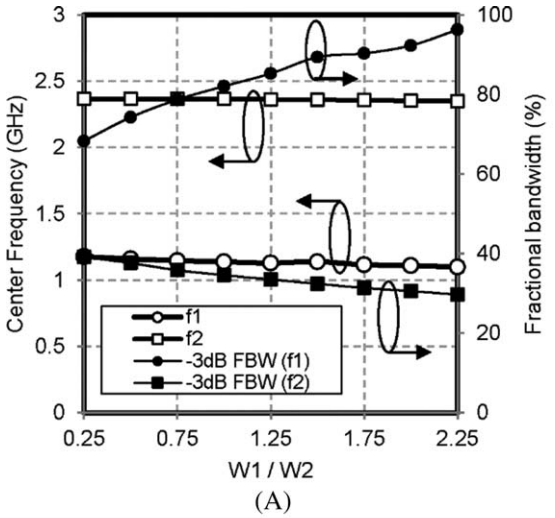

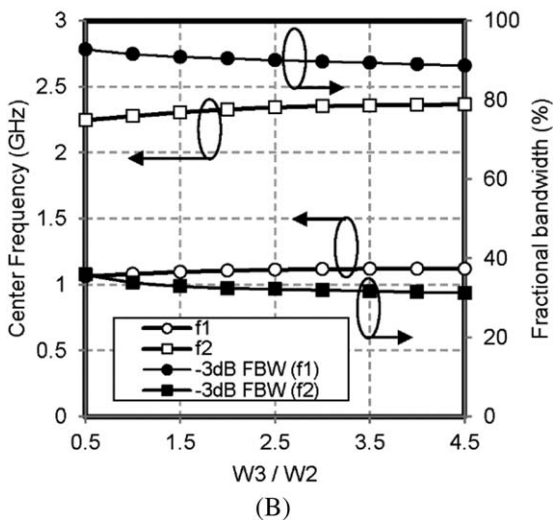

FIGURE 4 (A) The dependency of the center frequency and fractional bandwidth on the impedance ratio (W_1/W_2). (b) The stability of the center frequency and fractional bandwidth on the impedance ratio (W_3/W_2)

As a novelty in this letter, we propose a dual-wideband band pass filter (DW-BPF) using cross-stub stepped impedance resonator (CS-SIR). Figure 1 shows a CS-SIR which was used to replace the conventional half-wavelength open stub resonators. A folded CS-SIR (FCS-SIR) was also proposed to reduce the filter size. Thus, the BPF size is reduced to 53%. The proposed design could be validated by simulations and measurements. This letter is organized as follows: Section 2 briefly describes the design of the proposed DW-BPF using CS-SIR, Section 3 presents the simulated and experimental results, and finally, Section 4 concludes this research.

2 | PROPOSED DUAL-WIDEBAND BAND PASS FILTER

A half-wavelength open stub resonator structure was commonly used to design the conventional single-band

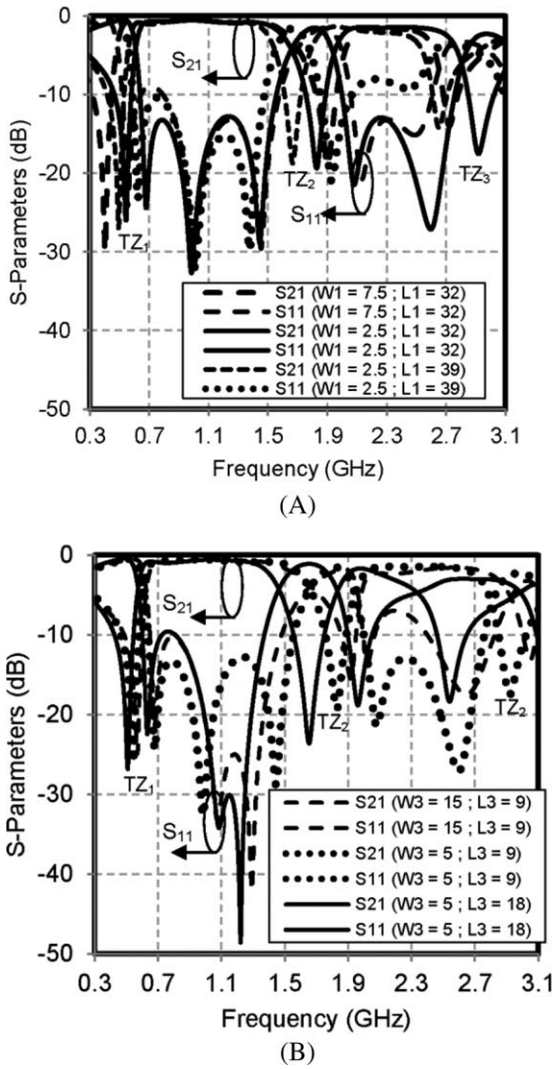

FIGURE 5 (A) Transmission coefficients (S_{21}) and reflection coefficients (S_{11}) response with varied W_1 and L_1. (B) Transmission coefficients (S_{21}) and reflection coefficients (S_{11}) response with varied W_3 and L_3

microstrip BPF.[1] In this letter, the half-wavelength open stub resonator is converted to the stub stepped impedance resonator as shown in Figure 1. The CS-SIR structure consists of three transmission lines having different characteristic impedances Z_N (N = 1,2,3) with corresponding electrical lengths θ_N (N = 1,2,3), respectively. Analyzing the input impedance $Z_{IN(SIR)}$ of the stepped impedance resonator section, the following equations can be derived:

$$Z_{IN(1)} = -jZ_1 \cot\theta_1 \tag{1}$$

$$Z_{IN(2)} = Z_2 \frac{Z_{IN(1)} + jZ_2 \tan\theta_2}{Z_2 + jZ_{IN(1)} \tan\theta_2} \tag{2}$$

$$Z_{IN(SIR)} = Z_{IN(3)} = Z_3 \frac{Z_{IN(2)} + jZ_3 \tan\theta_3}{Z_3 + jZ_{IN(2)} \tan\theta_3} \tag{3}$$

Equation (3) can also be expressed as:

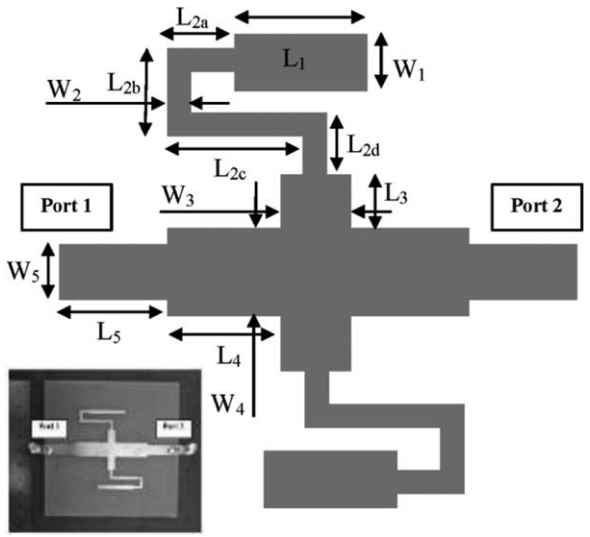

FIGURE 6 The layout and photograph of the design DW-BPF using folded CS-SIR (FCS-SIR)

$$Z_{IN(SIR)} = Z_1 \frac{Z_2(-jZ_3\cot\theta_3 + jZ_2\tan\theta_2) + jZ_1\tan\theta_1(Z_2 + Z_3\cot\theta_3\tan\theta_2)}{Z_1Z_2 + Z_1Z_3\cot\theta_3\tan\theta_2 + Z_2Z_3\cot\theta_3\tan\theta_1 - Z_2^2\tan\theta_2\tan\theta_1} \tag{4}$$

The resonant frequencies can be extracted from admittance condition $Y_{IN(SIR)} = 0$ or impedance condition $Z_{IN(SIR)} = \infty$.[1] This can be obtained when:

$$Z_2^2\tan\theta_3\tan\theta_1\tan\theta_2 - Z_1Z_2\tan\theta_3 - Z_1Z_3\tan\theta_2 - Z_2Z_3\tan\theta_1 = 0 \tag{5}$$

with the Z_N (N = 1,2,3) and θ_N (N = 1,2,3) stand for the characteristic impedance and electrical length, respectively. For the same electrical length $\theta_1 = \theta_2 = \theta_3 = \theta$, the resonance condition can also be shortened as follows:

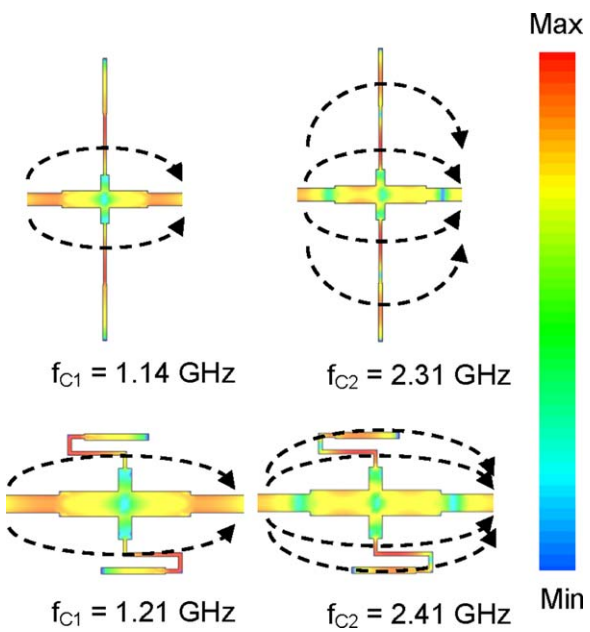

FIGURE 7 The surface current of the DW-BPF with CS-SIR and FCS-SIR. [Color figure can be viewed at wileyonlinelibrary.com]

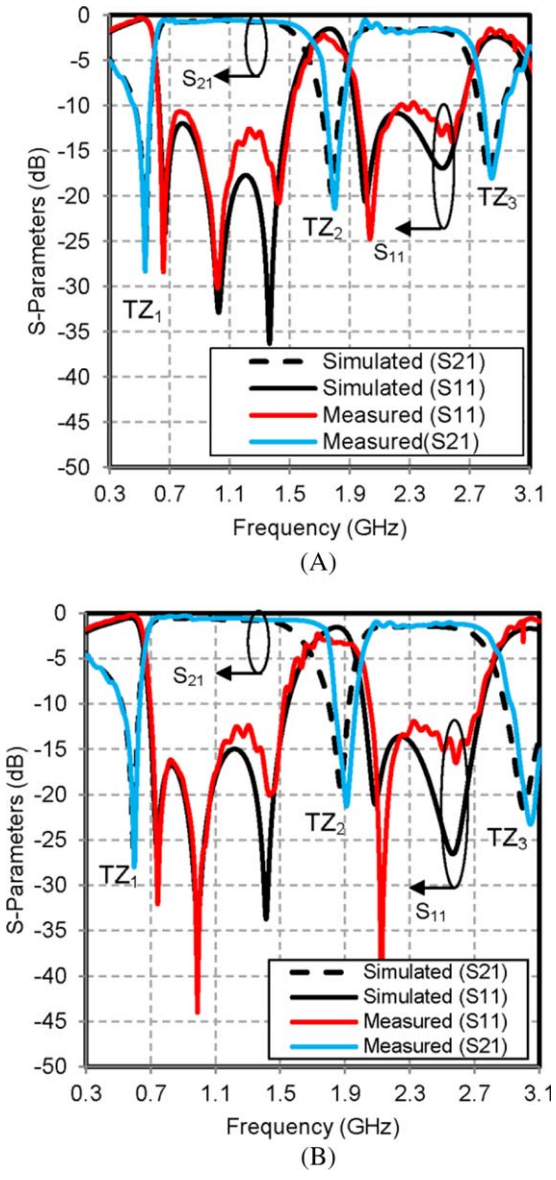

FIGURE 8 (A) Comparison between simulated and measured results of DW-BPF using CS-SIR. (B) Comparison between simulated and measured results of DW-BPF using FCS-SIR. [Color figure can be viewed at wileyonlinelibrary.com]

$$\tan^3\theta - K_1\tan\theta - K_1K_2\tan\theta - K_2\tan\theta = 0 \tag{6}$$

which can also be expressed as:

$$\tan\theta\ \left(\tan\theta + \sqrt{K_1 + K_1K_2 + K_1}\right)\left(\tan\theta\ - \sqrt{K_1 + K_1K_2 + K_1}\right) = 0 \tag{7}$$

where the impedance ratio K_N (1,2) is defined by:

$$K_1 = \frac{Z_1}{Z_2}, \text{ and} \tag{8}$$

$$K_2 = \frac{Z_3}{Z_2} \tag{9}$$

respectively. Equation (4) shows that the resonator provides two resonating frequencies. Therefore, the resonator serves as a dual mode resonator to produce two resonant frequencies. The relationship of K_1, K_2, and θ is shown in Figure 2.

3 | RESULTS AND DISCUSSION

Figure 3 shows the schematic of the design DW-BPF using CS-SIR. The DW-BPF was fabricated on microstrip with $\varepsilon_r = 4.4$, $h = 0.8$ mm, and $\tan\delta = 0.0265$. The DW-BPF consists of input/output port (*I*/*O*) line and two stub-SIR placed in a crossed manner. The DW-BPF was simulated using advanced design system (ADS) software, whereby an RS-ZVA vector network analyzer (VNA) was used to test the fabricated prototype of DW-BPF. The dimensions are given as follows (all in millimeters): $L_1 = 32$, $L_2 = 35$,

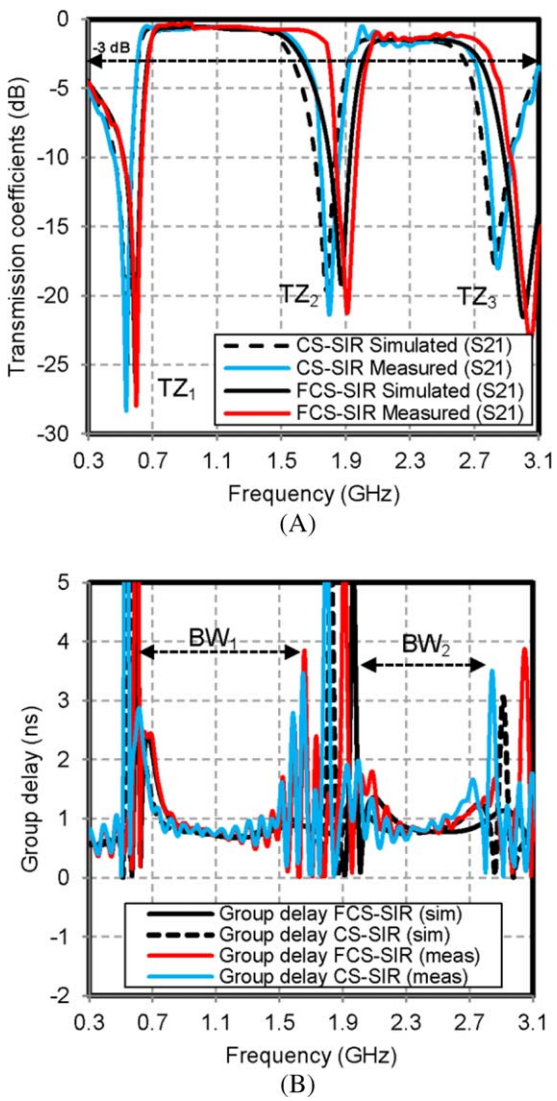

FIGURE 9 (A) Comparison of transmission coefficients (S_{21}) between DW-BPF using CS-SIR and DW-BPF using FCS-SIR. (B) Comparison of group delays (GDs). [Color figure can be viewed at wileyonlinelibrary.com]

TABLE 1 Summary of the proposed dual-wideband BPF comparison

Ref.	Method	Center frequency (GHz)	Transmission coefficients (dB)	–3 dB FBW (%)
[2]	Square loop dual mode resonator	3.45/6.65	0.70/1.20	14.49/8.27
[3]	Defected ground structure (DGS)	4.60/7.30	0.34/0.35	3.87/2.12
[4]	Defected ground spiral resonator	1.87/2.43	2.00/2.00	4.50/3.30
[5]	Four spiral resonators	1.80/2.40	1.6/2.5	5.60/3.00
[6]	Defected stepped impedance resonator (Defected-SIR)	2.35/3.15	0.50/1.5	3.90/2.80
[7]	Defected stepped impedance resonator (Defected-SIR)	1.85/2.35	0.50/1.00	5.50/4.50
[8]	Slotted stepped impedance resonator (Slotted-SIR)	2.40/3.50	1.80/2.9	4.10/1.40
[9]	Multilayer stepped impedance resonator (Multilayer-SIR)	2.45/5.80	1.35/0.98	3.06/2.16
[10]	Multilayer stepped impedance resonator (Multilayer-SIR)	2.40/5.20	1.20/1.50	5.40/7.30
[11]	Meandering stepped impedance resonators (Meandering-SIR)	2.40/5.25	0.72/2.10	8.33/3.85
[12]	Stub-loaded stepped impedance resonator (Stub-loaded SIR)	2.40/5.20	1.20/2.00	8.00/5.00
[13]	Coupled stepped impedance resonator (Coupled-SIR)	2.4/3.8	0.50/1.00	8.33/5.26
This Work	Cross-stub stepped impedance resonator (CS-SIR)	1.14/2.31	0.22/1.87	94.19/33.52
	Folded cross-stub stepped impedance resonator (FCS-SIR)	1.21/2.41	0.19/1.29	89.08/31.90

$L_3 = 9.0$, $L_4 = 23$, $L_5 = 21$, $W_1 = 2.5$, $W_2 = 1.5$, $W_3 = 5.0$, $W_4 = 10$, and $W_5 = 7.0$.

The dependency of the center frequency and fractional bandwidth on the impedance ratio (W_1/W_2) is given in Figure 4A. The figure shows that by increasing the impedance ratio (W_1/W_2), the center frequencies will be stable. However, increasing impedance ratio (W_1/W_2) would raise the fractional bandwidth. Figure 4B also shows the stability of the center frequency and fractional bandwidth on the variance of impedance ratio (W_3/W_2). The chart shows that both center frequency and fractional bandwidth were not changed significantly. Figure 5A and B shows transmission coefficients (S_{21}) and reflection coefficients (S_{11}) in response to varied W_1, W_3, L_1, and L_3.

In order to reduce the filter size, a folded CS-SIR (FCS-SIR) was proposed as shown in Figure 6. The dimensions are given as follows (all in millimeters): $L_1 = 32$, $L_{2a} = 5$, $L_{2b} = 5$, $L_{2c} = 20$, $L_d = 5$, $L_3 = 9.0$, $L_4 = 23$, $L_5 = 21$, $W_1 = 2.5$, $W_{2a} = W_{2b} = W_{2c} = W_{2d} = 1.5$, $W_3 = 5.0$, $W_4 = 10$, and $W_5 = 7.0$. As a result, this BPF size was reduced to 53%. Furthermore, both DW-BPF using CS-SIR and folded CS-SIR (FCS-SIR) were accomplished with two pass bands. Figure 7 shows the surface current at filter with CS-SIR and FCS-SIR. It shows that the first center frequency will obtain maximum value of surface current at transmission line 2 (W_2, L_2) and the second center frequency will obtain maximum value of surface current at transmission line 1 (W_1, L_1) and transmission line 3 (W_3, L_3).

Figure 8A shows a comparison between simulated and measured of DW-BPF using CS-SIR. A DW-BPF with CS-SIR achieves transmission-coefficients/fractional-bandwidth of 0.22 dB/94.19% and 1.87 dB/33.52% at 1.14 GHz and 2.31 GHz, respectively. The transmission zeros (TZ) of this filter are −28.29 dB, −21.36 dB, and −18.02 at 0.53 GHz, 1.79 GHz, and 2.86 GHz, respectively. Furthermore, Figure 8B shows a comparison between simulated and measured of

DW-BPF using FCS-SIR. A DW-BPF with FCS-SIR achieves transmission coefficients/fractional bandwidth of 0.19 dB/89.08% and 1.29 dB/31.90% at 1.21 GHz and 2.41 GHz, respectively. The transmission zeros (TZ) of this filter are −27.94 dB, −21.25 dB, and −23.25 at 0.59 GHz, 1.90 GHz, and 3.04 GHz, respectively. Figure 9A shows a comparison of transmission coefficients (S_{21}) between DW-BPF using CS-SIR and DW-BPF using FCS-SIR. The measured group delays (GDs) of all pass bands below 5 ns are also depicted in Figure 9B. Table 1 summarizes the comparison of the proposed dual band BPF. Finally, the measured results are in a very good agreement with the simulated results.

4 | CONCLUSION

This letter proposes a dual-wideband band pass filter (DW-BPF) using cross-stub stepped impedance resonator (CS-SIR). The CS-SIR was used to replace the conventional half-wavelength open stub resonators. In order to reduce the filter size, a folded CS-SIR (FCS-SIR) also was proposed. As a result, this BPF size is reduced to 53%. Measured results are in a very good agreement with the simulated results. In comparison with the previous works, both of BPF using CS-SIR and BPF using FCS-SIR could produce wider bandwidth, good transmission coefficients, and ease of fabrication.

ACKNOWLEDGMENTS

The work for this grant was supported by the Ministry of Research, Technology and Higher Education, Indonesian Government in Penelitian Kerjasama Perguruan Tinggi (Grand No. 267/UN43.9/PL/K/2016).

REFERENCES

[1] Alkanhal MAS. Dual-band bandpass filters using inverted stepped-impedance resonators. *J Electromagn Waves Appl.* 2009;23:1211–1220.

[2] Atallah B, Jan M, And AB. Dual-band bandpass filter by using square-loop dual-mode resonator. *Microwave Opt Technol Lett.* 2008;50:1567–1570.

[3] Shervin A, Mahboubeh K. Improvement the design of microwave dual-band BPF by DGS technique. *Microw Opt Technol Lett.* 2016;58:2133–2137.

[4] Mi X, Guoliang S, Fang X. Compact dual-band bandpass filters based on a novel defected ground spiral resonator. *Microw Opt Technol Lett.* 2016;58:1636–1640.

[5] Hung C-Y, Yang R-Y, Lin Y-L. A simple method to design a compact and high performance dual-band bandpass filter for GSM and WLAN. *Prog Electromagn Res C.* 2010;13:187–193.

[6] Bian W, Chang-Hong Liang L, Qi L, Pei-Yuan Q. Novel dual-band filter incorporating defected SIR and microstrip SIR. *IEEE Microw Wireless Comp Lett.* 2008;18:393–394.

[7] Bian W, Chang-Hong Liang L, Pei-Yuan Q, Qi L. Compact dual-band filter using defected stepped impedance resonator. *IEEE Microw Wireless Comp Lett.* 2008;18:674–676.

[8] Lan S, Xuehui G, Xiaoyan Z. Compact dual-mode dual-band bandpass filter using slotted stepped-impedance resonator. *Microw Opt Technol Lett.* 2016;58:1056–1060.

[9] Djaiz A, Nedil M, Habib AM, Denidni TA. Compact multilayer dual-band filter using slot coupled stepped-impedance-resonators structure. *Microw Opt Technol Lett.* 2009;51:1635–1638.

[10] Min-Hang Weng W, Ru-Yuan Y, Yu-Chi Chang C, Hung-Wei Wu W, Kevin S. Design of a multilayered dualband bandpass filter with transmission zeros. *Microw Opt Technol Lett.* 2008;50:2010–2013.

[11] Fu-Chang C, Qing-Xin C. Filter using meandering stepped impedance resonators. *Microw Opt Technol Lett.* 2008;50:2619–2612.

[12] Mingqi Z, Xiaohong T, Fei X. Compact dual band transversal bandpass filter with multiple transmission zeros and controllable bandwidths. *IEEE Microwave Wireless Comp Lett.* 2009;19:347–349.

[13] Changsoon K, Tae Hyeon L, Bhanu S, Kwang Chul S. Miniaturized dual-band bandpass filter based on stepped impedance resonators. *Microw Opt Technol Lett.* 2017;59:1116–1119.

How to cite this article: Firmansyah T, Praptodinoyo S, Wiryadinata R, et al. Dual-wideband band pass filter using folded cross-stub stepped impedance resonator. *Microw Opt Technol Lett*. 2017;59:2929–2934. https://doi.org/10.1002/mop.30848

Received: 16 April 2017

DOI: 10.1002/mop.30847

A new filter antenna using improved stepped impedance hairpin resonator

Dan Feng | Huiqing Zhai | Lei Xi | Kedi Zhang | Dong Yang

National Key Laboratory of Antennas and Microwave Technology, School of Electronic Engineering, Xidian University, Xi'an, Shaanxi 710071, China

Correspondence
Huiqing Zhai, National Key Laboratory of Antennas and Microwave Technology, School of Electronic Engineering, Xidian University, Xi'an, Shaanxi 710071, China.
Email: hqzhai@mail.xidian.edu.cn

Abstract

In this letter, a filter antenna based on novel wide stop-band low-pass filter has been presented. The introduction